Title

Spectroscopic Properties of Gold Nanoparticles at the Single-Particle Level in Biological Environments

Journal

ChemPhysChem, 13(4)

ISSN

1439-4235

Authors

Estrada, Laura C

Gratton, Enrico

Publication Date

2012-03-01

DOI

10.1002/cphc.201100771

Published in final edited form as:
Chemphyschem. 2012 March ; 13(4): 1087–1092. doi:10.1002/cphc.201100771.

Spectroscopic properties of gold nanoparticles at the single particle level in biological environments

Laura C. Estrada, PhD[*] and **Enrico Gratton, PhD**[*]
Laboratory for Fluorescence Dynamics, Biomedical Engineering Department, University of California, Irvine, USA, 3311 Natural Sciences II, Irvine, CA 92697-2715, USA

Abstract

Labeling cells and tissues with fluorescent probes such as organic dyes and quantum dots (Qdots) is a widespread and successful technique for studying molecular dynamics both in vitro and in vivo. However, those probes usually suffer from underisable photophysical/photochemical processes, such us blinking and photobleaching, limiting their utilization. The main challenges in fluorescent probe design are to improve their absorption/emission properties, and to provide higher stability against photobleaching. In the last few years, metallic nanoparticles (NPs) of various sizes, shapes, and compositions have been used as a new alternative for cellular microscopy. This is in part because –unlike common organic dyes and Qdots– metallic NPs do not bleach or blink upon continuous illumination, are extremely stable, very bright, and their luminescence spans over the visible spectrum. These characteristics make them an attractive contrast agent for cell imaging both in vitro and in vivo. For these reasons, the emission of metallic NPs in bulk solutions has already been extensively characterized. In contrast with bulk experiments, where billions of molecules are measured simultaneously, single particle techniques allow the observation of characteristics and dynamical processes otherwise hidden in the measured average. A full understanding of the photophysical properties of the NPs is critical when they are used for single-molecule applications. Photophysical processes can be a source of artifacts if they are not interpreted accordingly and thus a careful characterization of these labels at the single particle level became crucial for the correct interpretation of the experimental results. In this work we study some of their unique optical properties at the single particle level, and show examples that illustrate their intrinsic heterogeneity when used in biological environments.

Keywords

fluorescence microscopy; luminescence; nanoparticles; photophysics; two-photon microscopy

Introduction

Metallic nanoparticles (NPs) of various sizes, shapes, and compositions have recently become popular as new labels for microscopy. This is in part because, unlike common fluorescent probes such as organic dyes and quantum dots, metallic NPs do not photobleach

Fax: +1-949-824-1727, egratton22@yahoo.com, laura.estrada@uci.edu.
Supporting information for this article is available on the WWW under http://www.chemphyschem.org or from the author.

or blink upon continuous illumination.[1] Furthermore, the understanding of the chemistry of metallic NPs allows us to synthesize them in different shapes and sizes with good reproducibility. One of the main interests in using NPs is that they can confine the excitation energy in small regions near the NP surface producing strong enhanced fields. These enhanced fields have been used in a wide range of applications such as Surface Enhanced Raman Scattering,[2, 3, 4] high spatial resolution probes for microscopy,[5, 6] near field correlation spectroscopy,[7] and nanoscale plasmonic devices.[8, 9, 10] More recently, a 2-photon excitation microscope has been used to move single gold NPs along actin filaments within Chinese Hamster Ovary (CHO K1) living cells [11] where its three-dimensional trajectory provides the topography of the fiber with nanometer resolution.

Numerous examples can be found in literature where these labels, depending on their sizes, can be detected by their scattering, absorption, or more generally by their luminescence.[1, 12, 13, 14, 15, 16] It has been demonstrated that Multiphoton-Absorption-Induced Luminescence from gold NPs is efficiently generated using a 2-photon excitation source at 800 nm with excitation intensities that are lower than those typically used for 2-photon imaging of living cells.[1] 25 years ago, Boyd and co-workers showed that gold surfaces exhibit ~100 times more luminescence when irradiated with a 2-photon excitation source compared to 1-photon excitation.[16] In the case of gold and silver NPs it has also been shown that their luminescence spans over the visible spectrum and was demonstrated to arise, depending on the excitation intensities used, from a multi-photon absorption effect.[12, 17] In recent years, several authors have proposed interesting applications of NP's photoinduced luminescence. In 2007, Durr and collaborators have shown that, when irradiated at 760 nm, the 2-photon luminescence from cancer cells targeted with gold nanorods is 3 orders of magnitude brighter than the 2-photon autofluorescence signal from the unlabeled cells.[15] In 2005, Wang et al. imaged single gold nanorods flowing in mouse ear blood vessels within cancer cells.[18] The potential application of the luminescence from silica/gold hybrids nanoshells for biological imaging was demonstrated by recording the three dimensional distribution of the hybrids within murine tumors.[19]

Clearly, 2-photon induced luminescence from metallic nanostructures has attracted the attention of many researchers. Their excellent optical and chemical properties make them an attractive contrast agent for cellular imaging both in vitro and in vivo. However, in spite of the fact that interesting applications were already shown in literature,[20, 21] a clear and general understanding of the photophysical/photochemical luminescence's properties is not yet available. In the last year, different theoretical models have been proposed to understand the emission of these NPs.[22, 23] However, because photophysical processes that can occur at the single particle level such as photodegradation or blinking produce results that can be misinterpreted, a careful study of NPs properties is critical for the correct interpretation of the experimental results. Experimentally, the challenge is to develop a method to spectroscopically characterize metallic nanostructures within living cells and at the single particle level.

The Orbital Tracking Method (OTM) developed in our lab some time ago[24] allows us to simultaneously track single NPs and spectroscopically characterize their emission while moving in three-dimensions inside cells. In the OTM the observation volume of a 2-photon

or confocal microscope, orbits around a moving NP keeping it centred via a feedback algorithm (see Figure in table of contents). This approach brings some advantages in comparison with the image-based single particle tracking techniques. As has been already shown,[25] the OTM has a very high spatio-temporal resolution (1-50 nm, depending on number of collected photons; and 1-30 ms depending on the time response of the galvano/piezo devices). More relevant to this work, the OTM is capable of measuring spectroscopic properties such as fluorescence lifetime, emission/absorption spectrum, or polarization from an object as it freely moves in three-dimensions. In this work, we used the OTM implemented on a 2-photon laser scanning microscope to study spectroscopic properties of single gold NPs ranging from 20 to 80 nm and exposed to different surroundings.

Results and Discussion

Gold nanoparticles: 2-photon microscopy and spectroscopic properties

Figure 1 shows 2-photon excitation images that were obtained on CHO K1 cells labeled with Alexa 488-phalloidin (Invitrogen, USA) and incubated overnight with 20 nm gold NPs (Ted Pella, USA). During incubation, cells uptake NPs from the medium and after that, a large number of particles are found inside the cells. However, during the imaging time (1hr/sample) NPs do not appear to harm the cells. A control sample (Figure 1A) was prepared in the same way but omitting the incubation with the NPs. We observed that the cells incubated with the gold NPs (Figures 1B and 1C) exhibit a stronger luminescence signal than those without NPs.

In Figure 2, 80 and 40 nm gold NPs electrostatically attached to polyethylenimine (PEI) coated coverslips (see Experimental Section) were irradiated using the excitation wavelengths of a Ti:Sapphire laser (Chameleon Ultra, Coherent Inc., USA) ranging from 750 nm to 860 nm and an excitation power of approximately 0.5 mW for all wavelengths. Each image in Figure 2A corresponds to the average of 10 consecutive frames and the bright spots correspond to the diffraction limited pattern of the 2-photon induced signal from single NPs. To positively identify those spots as individual NPs, we performed a spectral characterization taking advantage of the fact that the plasmon absorption of metallic NPs is strongly dependent on the size, shape and NP composition. To do so a 1-photon excitation experiment was performed and the transmitted light was recorded and analyzed as discussed in a recent work[11]. Briefly, inspection of the images acquired using a 1-photon microscope shows diffraction limited bright spots that in principle could correspond to gold NPs. First, we measured a transmission image with each excitation line available in the microscope (405 nm, 472 nm, 449 nm, 488 nm, 543 nm, 633 nm). After that, for each spot in the image regarded as a NP, we calculated the corresponding background-corrected intensity value and obtained the normalized extinction values at the given wavelengths. Finally, we superimposed the obtained values with the extinction spectrum of a suspension of the same NPs. The data taken in the suspension and on individual spots of the transmission image agree very well, thus confirming that the spots in the images are indeed NPs of the same kind of those in the suspension. Once the NPs were identified as such, the samples were measured in the 2-photon microscope for further analysis.

The color scale in Figure 2A, was kept constant from 0 counts/16μs (dark blue) to 55 counts/16μs (red) and serves as an indicator of the NP's 2-photon luminescence. The difference in intensity seen among particles (even for those NPs inside the same field of view) is due to the local coupling of the laser beam with the glass substrate. So, these intensity differences do not reflect an intrinsic optical property of the particle itself but a "NP substrate" convolute property. We have observed this characteristic oscillatory signal in all the samples studied in this work regardless the NP's size. Figure 2B and C show typical "NP substrate combined" spectra for two different NPs sizes (80 and 40 nm in diameter). Analyzing different NPs inside the same field of view (meaning NPs where the excitation and acquisition parameters were kept constant), shows that the oscillatory behavior remained present in all the NPs regardless their size. To build up the NP substrate "combined" spectrum, ten images per excitation wavelength were acquired and changes in the collected intensity were recorded even within those images (images taken at the same excitation wavelength), meaning that the vicinity with the substrate has a measurable contribution in the detected signal. This substrate contribution completely disappears when the NPs are immersed in a media. Figure 3 shows the 2-photon excitation spectra of a single gold NP when embedded in a 3D collagen matrix (Figure 3A solid squares) and the 2-photon excitation spectra taken on a collagen fiber for comparison (Figure 3A open circles). All the NPs studied were measured 3 micrometers above the glass surface to avoid the substrate contribution. For this work we used collagen hydrogels prepared from collagen type I rat tail (BD Biosciences, USA) as is explained in the Experimental section. Both spectra were taken using exactly the same experimental conditions.

To determine the excitation dependence of the 2-photon luminescence emission, two methods were employed depending on the mobility of the NPs. If the NPs remained stationary during the acquisition time (the NP's displacement < ~400 nm), raster scan images were collected at 256×256 pixels with a 16 or 20 μs pixel dwell time. 5 to 10 frames per excitation wavelength were first averaged and then analyzed using SimFCS software (Laboratory for Fluorescence Dynamics, USA). To determine the intensity of the emitted luminescence we proceeded as follows: we selected a region of the image which corresponds to the NP position and built up the histogram of the average intensity. We repeated the same procedure for each excitation wavelength. Finally, and as a control, we performed the same analysis on a collagen fiber. Figures 3B and 3C show a scheme of the detection path and a typical image where the NP and the collagen fiber can be easily identified in channels 1 and 2 respectively. On the contrary, if the NP moves substantially during the acquisition time, the OTM was employed alike previously shown in[25] to built up the excitation spectra.

Finally, we studied the effect of the polarization of the excitation beam. To do so, the emission from gold NPs and fluorescent beads was measured at different settings of a half-wave plate that rotated the incident polarization (Figure 4 and Supporting Information). A strong modulation in the measured signal demonstrates that the luminescence is significantly sensitive to the incident polarization whereas there is no significant effect on the fluorescence from beads. In the polarization-series of images shown in Figure 4 (lower panel), some NPs (within circles) oscillate between a bright and a dark depending on the

polarization direction of the incident beam, while others (within squares) follow a different oscillation pattern (see movie in Supporting Information for more details). A control sample (upper panel) was prepared in the same way but replacing gold NPs by fluorescent beads (Molecular Probes, USA). As expected, we observed that fluorescent beads do not show polarization effects in the emitted signal. Further measurements will be required to determine the absolute degree of polarization and whether the particles emit via a single dipole or a degenerate dipole.

SEM Characterization of Gold NPs

The SEM images of commercial gold NPs of various sizes showed that the measured mean diameters were in good agreement with the diameters specified by the manufacturer. The diameter variance for individual NPs of 20, 40 and 80 nm was 10% below the nominal values. Larger variations were observed for NPs with nominal diameters of 5 nm.

Conclusions

We showed that the strong 2-photon luminescence signal from metallic NPs allows using these particles as bright labels in cells and with potential applications in tissue studies. Metallic NPs are non-bleaching, non-blinking and non-toxic[26] labels that can be used both for detection of specific localization and single particle tracking experiments. The non-toxic nature of these nanostructures is of great importance compared to other label-systems, for example the heavy metals used for quantum dots fabrication. We observed that the maximum intensity occurs at different excitation wavelengths for different particles in the same image. This difference among particles is due to the local coupling of the laser beam with the glass substrate when gold NPs attached onto PEI coated coverslips are imaged. This substrate contribution completely disappears when the NPs are immersed in a 3D collagen matrix meaning that the collected signal strongly depends on the NP's environment (in particular on the presence or absence of an interface. Finally, the polarization studies show that the NP's luminescence also depends on the NP's environment, suggesting the possibility of using these labels as sensors to study surface properties.

In summary, we have shown that luminescence from gold nanoparticles can be efficiently generated via the near-infrared excitation using a 2-photon excitation microscope and low excitation intensities. NPs are non-toxic for cells experiments and largely photostables. The luminescence spectral dependence on the excited wavelength and the luminescence polarization studies suggest the possibility of using these nanostructures as efficient tags for Surface Enhanced Raman Spectroscopy experiments among other surfaces studies. More importantly, the entire characterization has been performed at a single particle level allowing us to study dynamical aspects of NPs emission/absorption properties without the artifacts inherent to bulk experiments.

Experimental Section

Orbital Tracking Method

The Orbital Tracking Method (OTM) used in this work was developed by our group a few years ago.[24] Briefly, the OTM involves four main steps. First, a raster scan image is taken

in order to find a region where the particles to be tracked are clearly seen. After the particle has been chosen, we click on top of it to direct the position of the excitation beam by moving the galvano/piezo devices. Then, the beam performs a circular orbit with the previously chosen center. During each cycle of the orbital scanning, the intensity data is measured in 64, 128 or 256 points around the circular path. From the recorded intensities along the orbit, the tracking algorithm calculates the distance between the particle's position and the center of the initial orbit as described in detail in reference.[24] Finally, the center of the orbit is moved to the calculated position before the next cycle starts. The movements of the orbit center and the recovered particle's position from the previous cycle are displayed on the screen in real time.

2-photon microscope for Orbital Tracking

The excitation spectra of single gold NPs were measured using a home-built 2-photon excitation microscope based on an Olympus IX71 as described in detail in reference[25]. The same setup can be used either for measuring the excitation spectra, for measuring the emission spectra as also shown in[12, 25] or for tracking single NPs. The microscope was equipped with an Olympus UPlanFLN 60x air objective (NA=0.9) and two photomultipliers detectors with photon counting module (H7422P-40, Hamamatsu, Japan). The excitation light was provided by a mode-locked 80 MHz Ti:Sapphire laser (Chameleon Ultra, Coherent Inc., USA) with integrated Verdi tunable from 690 to 1040 nm. We used a short pass dichroic mirror (700DCSPXR, Chroma Technologies, USA) to direct the excitation light into the sample and a HQ700LP filter (Chroma Technologies, USA) to filter out the Ti:Sapphire fluorescence. The average laser irradiation after the microscope objective was measured with an Ultracompact laser power meter (New Focus Corp., USA), and was maintained below 1 mW in all experiments. Luminescence and/or Second Harmonic Generation (SHG) signals were detected through an emission filter (ET680SP, Chroma Technologies, USA) and split into two detectors using a dichroic mirror (485DCLP, Chroma Technologies, USA). Then, the SHG signal was spectrally filtered by a bandpass filter (HQ435/70, Chroma Technologies, USA) whereas no additional filters were used to detect the NP's 2-photon induced luminescence. After that the signal was amplified (ACA-4-35N, Becker&Hickl, Germany), and a constant fraction discriminator (model 6915; Phillips Scientific, USA) was used to convert the photon current in TTL electronic pulses. Finally, TTL pulses were counted using the FCS-PCI counter card (version 0.2, ISS, USA). The scanning of the samples was performed using galvano motor-driven mirrors (6350, Cambridge Technology Inc., USA) with controller series 603X servo system (60335 FM, Cambridge Technology Inc., USA), and a PIFOC P-721 piezo-driven objective device (Physik Instrumente, Germany). Both galvano and piezo were driven by an ISS 3-axis card (ISS, USA). Experiments were controlled by a commercially available data acquisition program (SimFCS, Laboratory for Fluorescence Dynamics, USA).

Scanning Electron Microscopy (SEM)

We used a scanning electron microscope (SUPRA™ 40 FESEM series, Carl Zeiss), to characterize the homogeneity of the nanoparticles used in this work. We recorded SEM images of various NP's sizes samples. The measured diameters showed that the NP's sizes are within specifications.

Nanoparticle's Sample Preparation

Before samples preparation, glass coverslips were immersed for 10 seconds in HF solution (5% w/w) and successively rinsed with Milli-Q water for 30 sec. After the cleaning process, coverslips were dried and stored in a close chamber until further use. For sample preparation, coverslips were treated with polyethylenimine (PEI) solution for 5 min (100 μL, 2% w/w), followed by three rinses with Milli-Q water. Finally, commercially available colloidal suspensions of gold NPs with nominal diameters of 80, 40, 5 nm (Ted Pella, USA) and 20 nm (EY laboratories, USA) were used. 50 μL of the suspension stock solution was placed on the surface of a previously cleaned and coated coverslip, incubated at room temperature for 5 min, and then rinsed with Milli-Q water for 30 sec. When completely dried, the samples were measured on the 2-photon excitation microscope previously described.

Fluorescent bead Sample Preparation

To acquire 2-photon images of fluorescent beads, glass coverslips were immersed for 10 seconds in HF solution (5% w/w) and successively rinsed with Milli-Q water for 10 sec. After the cleaning process, a 50 μL aliquot of the fluorescent beads stock solution (F8813, Molecular Probes, USA) was pipetted on top of the coverslip. Then, a 22 mm square coverslip was gently placed on the solution containing the bead. The second coverslip allows generating a very thin layer confining the fluorescent beads within a minimal thickness and reducing interference from out of focus beads.

Collagen Sample Preparation

The collagen hydrogel was prepared following the procedure detailed in reference[12]. Briefly, acid soluble rat tail tendon collagen type I (BD Biosciences, USA), Dulbecco's Modified Eagle's Medium (DMEM)-High Glucose (Sigma, USA), 5X DMEM (Sigma, USA) and 10X reconstitution buffer were placed on ice for at least half an hour prior to the preparation. NPs were sonicated for 15 minutes at room temperature. For each hydrogel sample, 30 μL of 10X reconstitution buffer, 60 μL of 5X DMEM, 64 μL of collagen type I high-concentration (concentration approximately 9 mg/ml) and 146 μL of DMEM-High Glucose were combined in that order and vortexed for 5 seconds. Finally, 30 μL of the NPs suspension was added and mixed into the hydrogel by gentle pipetting. Into each of the 10 mm diameter Lab-Tek Chamber slide (MatTek Corporation, USA), 330 μL of the gel mixture was pipetted and left to solidify at room temperature for at least 4 hours before imaging.

Cell measurements

For the studies performed in this work, Chinese Hamster Ovary (CHO K1) cells were used. Upon reaching 90% confluence, the cells were split using Phosphate Buffered Saline (PBS; Invitrogen, USA) Trypsin 1x (Invitrogen, USA) and plated onto fibronectin coated MatTek plates (P35G-1.5-14-C, MatTek Corporation, USA) with low glucose media supplemented with Fetal Bovine Serum (FBS; Invitrogen, USA), penicillin streptomycin, 1M hepes buffer and essential amino acids. For NPs endocytosis, cells media was removed and replaced by low glucose media. The cells were starved for two hours, and returned to complete media

containing 2 pM of gold NPs (Ted Pella, USA). Finally, they were incubated overnight at 37°C and 5% CO_2. Control samples without NPs were also prepared and no significant difference was seen suggesting that the NPs were not strongly affecting the cells. For cells imaging, actin staining was performed after NPs addition using Alexa Fluor 488 phalloidin (Invitrogen, USA) as it can be efficiently excited with a 2-photon excitation microscope. The stock solution of Alexa Fluor 488 phalloidin was prepared according to the manufacturer's indication. The cells were then incubated with a 1:100 dilution in PBS for 15 minutes, and afterwards washed three times with PBS. Finally, the cells were fixed using 4% paraformaldehyde (P6148, Sigma, USA).

Supplementary Material

Refer to Web version on PubMed Central for supplementary material.

Acknowledgments

This work is supported by the National Center for Research Resources division of the National Institutes of Health NIH-P41-RR003155, and the University of California, Irvine. We thank Silvio Ludueña, Claudia Marchi and the Centro de Microscopias Avanzadas, Facultad de Ciencias Exactas y Naturales, Universidad de Buenos Aires for their help with SEM images, and Milka Titin for her help with cells samples preparation.

References

1. Farrer RA, Butterfield FL, Chen VW, Fourkas JT. Nano Lett. 2005; 5:1139–1142. [PubMed: 15943457]
2. Sathuluri RR, Yoshikawa H, Shimizu E, Saito M, Tamiya E. PLoS ONE. 2011; 6(8):e22802. [PubMed: 21829653]
3. Talley CE, Jackson JB, Oubre C, Grady NK, Hollars CW, Lane SM, Huser TR, Nordlander P, Halas NJ. Nano Lett. 2005; 5(8):1569–1574. [PubMed: 16089490]
4. Tognalli N, Fainstein A, Calvo E, Bonazzola C, Pietrasanta L, Campoy-Quiles M, Etchegoin P. J Chem Phys. 2005; 123:044707. [PubMed: 16095384]
5. Scarpettini AF, Pellegri N, Bragas AV. Opt Commun. 2009; 282:1032–1035.
6. Anger P, Bharadwaj P, Novotny L. Phys Rev Lett. 2006; 96:113002. [PubMed: 16605818]
7. Estrada LC, Aramendía PF, Martínez OE. Opt Express. 2008; 16:20597–20602. [PubMed: 19065198]
8. Zou SL, Schatz GC. Phys Rev B. 2006; 74(12):125111.
9. Li KR, Stockman MI, Bergman DJ. Phys Rev Lett. 2003; 91:227402. [PubMed: 14683271]
10. Maier SA, Kik PG, Atwater HA, Meltzer S, Harel E, Koel BE, Requicha AAG. Nature Materials. 2003; 2(4):229–232.
11. Estrada LC, Gratton E. Nano Lett. 2011; 11(11):4656–4660. [PubMed: 21919444]
12. Chen B, Estrada LC, Hellriegel C, Gratton E. Biomed Opt Express. 2011; 2:511–519. [PubMed: 21412457]
13. Dowling MB, Li L, Park J, Kumi G, Nan A, Ghandehari H, Fourkas JT, Shong PD. Bioconjugate Chem. 2010; 21:1968–1977.
14. Lin A, Hoon Son D, Ahn IH, Hugh Song G, Won-Taek Han. Opt Express. 2007; 15:6374–6379. [PubMed: 19546942]
15. Durr NJ, Larson T, Smith DK, Korgel BA, Sokolov K, Ben-Yakar A. Nano Lett. 2007; 7:941–945. [PubMed: 17335272]
16. Boyd GT, Yu ZH, Shen YR. Phys Rev B. 1986; 33:7923–7936.
17. Kempa T, Farrer RA, Giersig M, Fourkas JT. Plasmonics. 2006; 1:45–51.

18. Wang HF, Huff TB, Zweifel DA, He W, Low PS, Wei A, Cheng JX. PNAS. 2005; 102:15752–15756. [PubMed: 16239346]
19. Park J, Estrada A, Sharp K, Sang K, Schwartz JA, Smith DK, Coleman C, Payne JD, Korgel BA, Dunn AK, Tunnell JW. Opt Express. 2008; 16:1590–1599. [PubMed: 18542237]
20. Qu XC, Wang J, Yao CP, Zhang ZX. Chin Opt Lett. 2008; 6:879–881.
21. Nagesha D, Laevsky GS, Lampton P, Banyal R, Warner C, DiMarzio C, Sridhar S. Int J Nanomed. 2007; 2:813–819.
22. Wu Z, Jin R. Nano Lett. 2010; 10(7):2568–2573. [PubMed: 20550101]
23. Beversluis MR, Bouhelier A, Novotny L. Phys Rev B. 2003; 68:115433.
24. Kis-Petikova K, Gratton E. Microsc Res Tech. 2004; 63(1):34–49. [PubMed: 14677132]
25. Hellriegel C, Gratton E. J R Soc Interface. 2009; 6(0 Suppl 1):S3–S14. [PubMed: 18753123]
26. Connor EE, Mwamuka J, Gole A, Murphy CJ, Wyatt MD. Small. 2005; 1:325–7. [PubMed: 17193451]

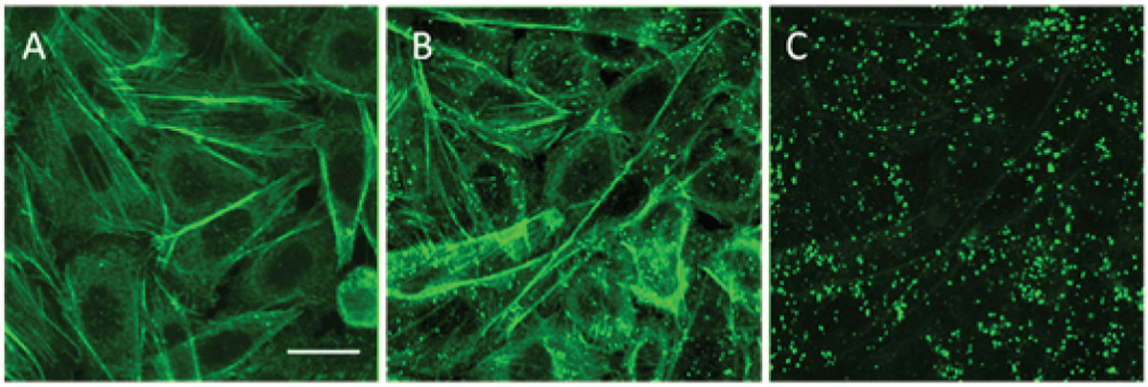

Figure 1.

CHO K1 cells stained with Alexa 488-phalloidin (Invitrogen, USA). (A) Control: Cells not exposed to NPs incubation. Excitation wavelength 780 nm; (B) 20 nm gold NPs (EY Laboratories, USA). Excitation wavelength 780 nm (C) 20 nm gold NPs (EY Laboratories, USA). Excitation wavelength 840 nm. Scale bar = 20 μm.

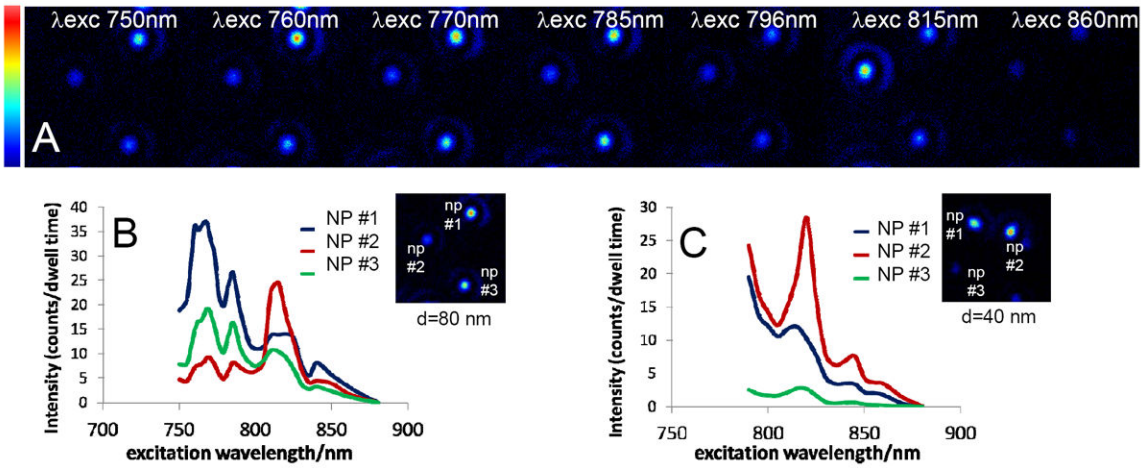

Figure 2.

gold NPs attached to PEI coated coverslips irradiated using the excitation wavelengths of a Ti:Sapphire laser. (A): the bright spots correspond to the diffraction limited pattern of the 2-photon induced signal from 80 nm single gold NPs. The image size is 7 μm and the color scale ranges from 0 counts/16μs (dark blue) to 55 counts/16μs (red). (B) and (C): NP substrate combined spectra for 80 and 40 nm diameter gold NPs. The spectra have an oscillatory behavior which is due to the coupling of the laser to the glass substrate rather than to an intrinsic property of the NPs.

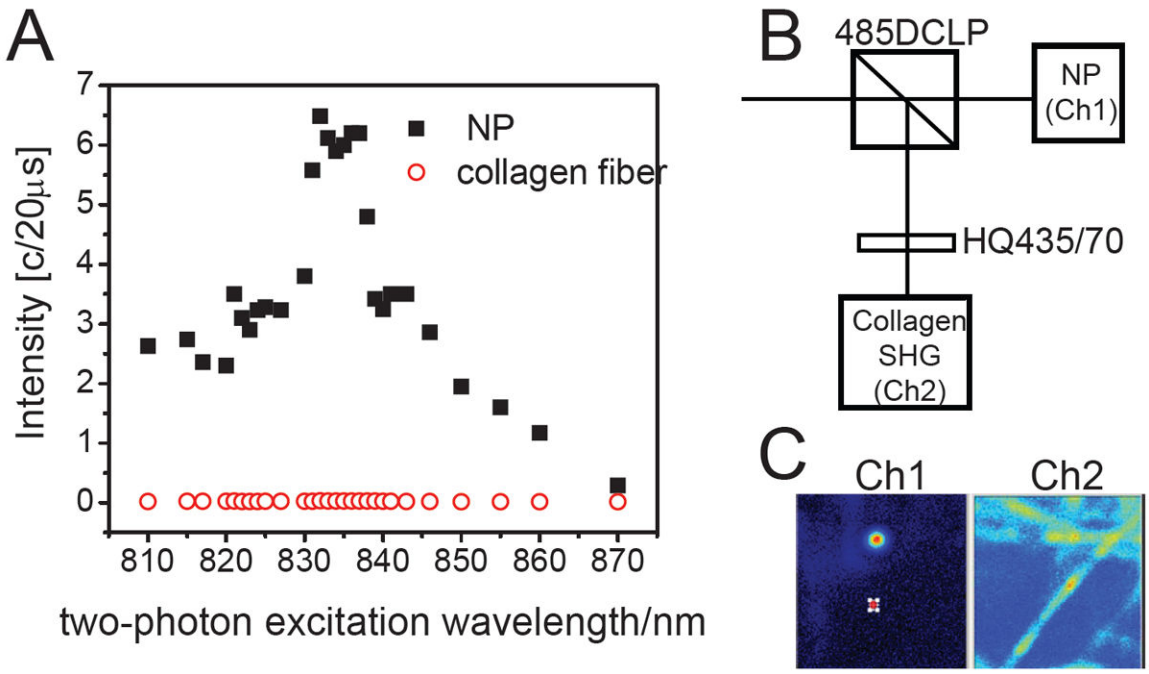

Figure 3.

(A) 2-photon excitation spectra from 20 nm gold nanoparticles embedded in a collagen fiber (solid squares), and the collagen fiber alone (open circles); (B) schematic representation of the detection path; (C) typical 2-photon excitation images from channel 1 (NP luminescence) and channel 2 (collagen second harmonic signal). The red spot in channel 1 shows the position where the collagen spectrum in panel (A) (open circles) was taken.

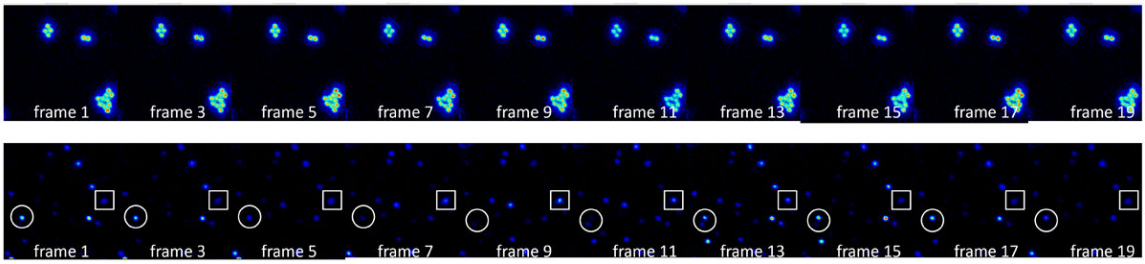

Figure 4.

Polarization-dependent spectroscopic properties of fluorescent beads (upper panel) and gold nanoparticles (lower panel) while changing the polarization direction of the incident beam. The excitation wavelength was set at 840 nm for gold NPs and 790 nm for fluorescent beads.